Microencapsulation yield assessment using TGA

Carlos García Carmona[1,2], Manuel J. Lis Arias[2], Oscar Garcia Carmona[2], Fabricio Maestá Bezerra[3], Marc Pallarès Andreu[1], Noelia de la Cruz Díaz[1].

[1]*GDE I+D+I, C/ Colom 564 Nau 1, 08228, Terrassa (Barcelona); cgc@gde7.com (C.G.C.); mpa@gde7.com (M.P.A.); ncd@gde7.com (N.C.D)*

[2]*Chemical Engineering Dept. ESEIAAT. UPC. Campus de Terrassa, Edificio TR1. C. Colom, 1, 08222, Terrassa;*
carlos.garcia.carmona@gmail.com (C.G.C.); manuel-jose.lis@upc.edu (M.L.A.); oscargarciacarmona@gmail.com (O.G.C.)

[3]*Federal University of Technology – Parana´, 635 Marcilio Dias Street, Apucarana, Parana´, Brazil;*
fabriciom@utfpr.edu.br

In this study, microcapsules containing different contents of different kinds of fragrances and with a regular spherical shape, 2,0–8,0 μm diameter, were synthesized in various core:shell ratios. Mint and cuir fragrances were successfully encapsulated in poly(urea-formaldehyde) (PUF) shell via in-situ polymerization. This was confirmed by optical microscope, scanning electron microscope (SEM) and Fourier transform infrared spectroscopy (FTIR) studies. By observation from thermogravimetric analysis (TGA), it was found a relation between thermal gravimetric curves and the amount of fragrance encapsulated, which was later contrasted by ultraviolet-visible spectroscopy. In this way, comparatively, the yield percentage values can be quantitatively defined with a sufficient degree of accuracy by TGA method.

1. Introduction

A typical cell in nature contains several types of organelles. These compartments, which are mostly surrounded by a single bilayer phospholipid membrane, each fulfill a unique role within the cellular environment. Different organelles comprise different collections of specific enzymes that catalyze requisite chemical reactions.

The process of compartmentalization to ensure the integrity of catalytic pathways has inspired chemists to mimic nature and create artificial environments for reactions to take place in. Liposomes, as pioneered by Bangham, were the first artificial capsules designed for this purpose. These structures are composed of phospholipids, which spontaneously assemble into a bilayer membrane architecture, similar to natural vesicles [1], [2]. Liposomes have been subject of extensive studies for decades already.

In recent years a different type of vesicular architecture, composed of macromolecules instead of small organic compounds, has become topic of investigation. A wide variety of polymeric capsules has been developed [3], [4].

One of the uses of these polymeric capsules is to control the release of volatile bioactive molecules, such as fragrances.

1.1. Fragrances

Fragrances are highly volatile compounds that have a pleasant odor [5], [6]. For an optimum performance of perfumed consumer articles, fragrances have to be protected against degradation and/or premature evaporation during storage, and to be released in a way to obtain a long-lasting fragrance perception after application.

One of the most common applications for the fragrances is in the fabric softeners. It is used to enrich our clothes and other fabrics with a lovely touch and fresh smell. The latest novelty in fabric softener land is the microcapsule. The idea of choosing mint and cuir fragrances was to apply aromatherapy so that the softeners manufactured with these microcapsules were a special, new product, since there are no softeners of mint or cuir fragrances commercially available.

1.2. Microparticles

To achieve high storage stability and to provide a slow (or at least controlled) release of the fragrance(s) in application, a number of perfume delivery systems have been developed. The polymer-based fragrance delivery systems rely on encapsulation of the fragrance in an appropriate particle or capsule [7]-[9]. To this end, a variety of systems has been explored, including linear or branched random or block copolymers [10]-[13], core–shell capsules [14]-[18], and nanoparticles [19], [20].

The formed microparticles are categorized as either microcapsules or microspheres (Figure 1), based on the structure, or more precisely, the mutual position of the core and the shell. In a microcapsule, the active ingredient is a continuous, concentrated phase and enveloped by a protective layer of coating material. Usually a two-step process will be needed to produce microcapsules, including the formation of the core particles followed by a coating process. In contrast, in a microsphere, the active substance is dispersed in the structure and entrapped within the matrix material, which sometimes only involves a single-step of entrapment [21]. Microcapsules or microspheres may have diameters ranging from a few microns to a few millimeters.

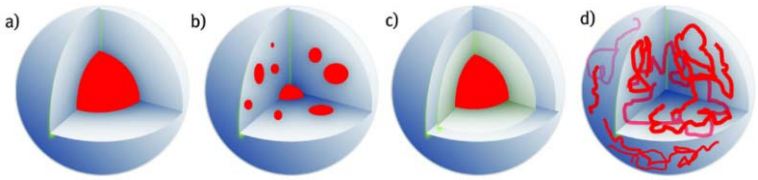

Figure 1. Microcapsules morphologies: (a) continuous core/shells, (b) polycore capsules and (c) continuous core capsules with more than one layer of shell material; Microspheres morphologies: (d) the matrix type capsules.

The different morphologies/species and even subspecies obtained can be of particular importance for the aim of this review which is not to give an overview of the different methodologies that can be utilized to form the various polymeric capsules that are known to control the release of fragrances, but rather to try to estimate the amount of oil encapsulated within these macromolecules by a comprehensive analysis from thermogravimetric analysis.

1.3. Thermogravimetry

Thermogravimetry involves the continuous recording of mass versus temperature (or time) as a sample is heated in a furnace with a controlled environment. The sample may be heated at a constant rate or held at an isothermal temperature. The era of modern automated

thermogravimetry started with the introduction of the electrobalance by Cahn and Schultz [22]. Other competitors, such as Mettler introduced their products in rapid succession. The components of the instrument are the microbalance, the furnace, the programmer controller, and a computer or data acquisition system.

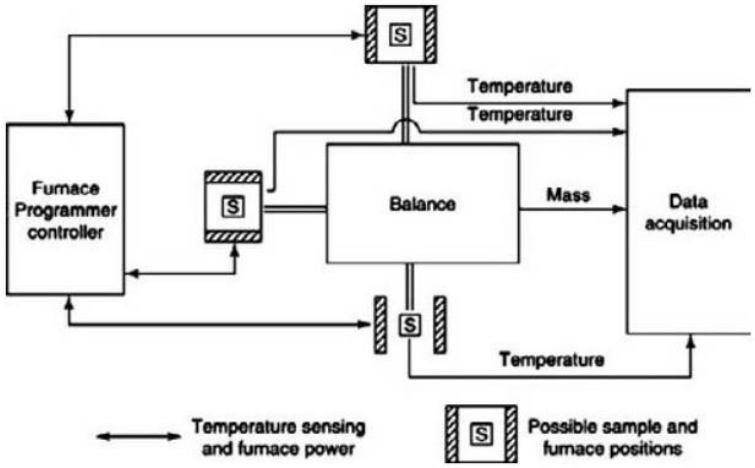

Figure 2. Typical arrangement for the components of a TGA instrument.

The principal applications of TGA/dTGA in polymers are determination of the thermal stability of polymers [23], compositional analysis [24], identification of polymers from their decomposition pattern [25] and to determine the kinetics of thermal decomposition. Also, in microencapsulation, TGA curves are used to verify that microencapsulation has been carried out [26]-[28]. However, the use of TGA as quantitatively analysis of encapsulation yield is still not known.

2. Experimental

2.1. Materials

Urea and formaldehyde (37 wt% aqueous solution) were purchased from Panreac, ethylene maleic anhydride (EMA) were purchased from Sigma Aldrich, Ammonium chloride and a hardener was supplied by Panreac, sodiumhydroxide and citric acid were bought from Merck Millipore and were used to control the pH of the reaction, fragrances were analytical grade reagent.

2.2. Synthesis of PUF-fragrance microcapsules

2.2.1. Pre-polymer preparation

PUF resins are traditionally produced by reaction of urea and formaldehyde (aqueous formaldehyde solution) in two stages, the first, addition, in slightly alkaline medium, the second, condensation, in acid medium:

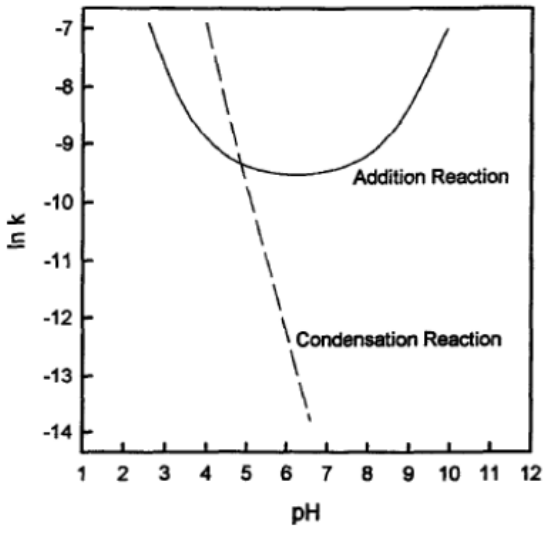

Figure 3. Addition and condensation reactions. Influence of pH [29].

A mixture of hydroxymethylureas species of the mono, di, and trisubstituted type, as well as oligomeric molecules is obtained by addition reaction between urea and formaldehyde (hydroxymethylation). The reaction is developed in basic medium and with a careful control of the pH, since the methyl-ol derivatives quickly condense in acidic medium as shown in the Figure 4:

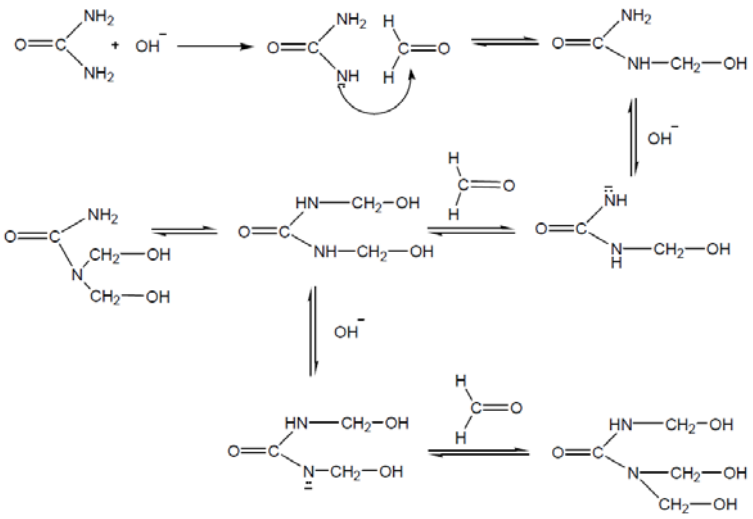

Figure 4. Hydroxymethylation reaction [29].

Condensation reaction between the hydroxymethylurea species originates prepolymers, through the formation of aminomethylene bonds, in addition to the ether type bonds. This stage can be considered as the critical of the process. The formation of the aminomethylene bonds must be favored with respect to the ether, since these are responsible for the emission of formaldehyde. In addition, the degree of condensation must be controlled, because a higher degree of condensation produces high molecular weight resin molecules, which decrease their solubility in water:

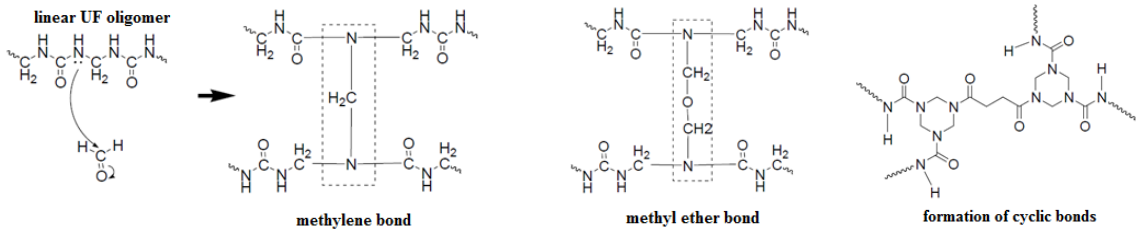

Figure 5. Different types of bonds that can be produced [29].

2.2.2. Methodology

PUF-fragrance microcapsules were synthesized through in-situ polymerization of urea and formaldehyde in an oil-in-water emulsion [30]. Firstly, 30 g of urea and 30 mL of formaldehyde were mixed with the pH adjusted to 8–9. After 1 h reaction, under agitation at 300rpm and 70ºC, a transparent methylol urea prepolymer was obtained. Figure 6 is a schematic representation of microcapsules produced by in-situ polymerization.

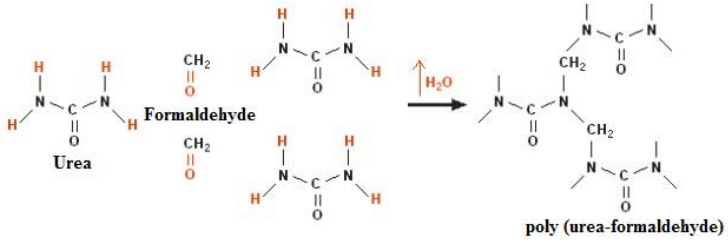

Figure 6. Chemical reaction involving shell wall formation [31].

Meanwhile, 1 g of EMA, 60 mL of fragrance, and a certain amount of deionized water were mixed at room temperature by stirring with a high-performance dispersing instrument (T-25, IKA) in a beaker to form stable oil in water emulsion for 30 min. The obtained microemulsion was added to the UF prepolymer prepared in the previous step into a 500ml five-necked round bottom flask, which was suspended in a temperature-controlled water bath at 60ºC. The pitched-blade impeller driven by an overhead mechanical stirrer was turned from 300 to 700 rpm to control the size of microcapsules. The pH of the solution was accurately adjusted to 4 by the addition of citric acid [32].

A refrigeration bath was placed just above the bottom of the flask to reduce the temperature until 15ºC for 90 min. Subsequently, 50 mL of hardener solution was added to the solution. After 12 h of agitation the mixer and bath were switched off and the system was neutralized to pH 7.

After the process finished, the suspension was filtered to collect the microcapsules. The obtained microcapsules were rinsed with ammonium chloride solution.

2.3. Characterization of PUF-fragrance microcapsules

2.3.1. Morphology of the microcapsules

The optical microscope (Motic BA310) was used to determine the size and distribution of the synthesized microcapsules. The mean diameter and size distribution of microcapsules were calculated by measuring more than 100 microcapsules using the software Image J. Surface morphology of microcapsules and their shell thickness were characterized using a scanning electron microscope (Jeol, JSM 5610).

2.3.2. Fourier transform infrared spectroscopy

The spectra of urea and the synthesized PUF-fragrance microcapsules were recorded with a Shimadzu 8400S Infrared spectrophotometer to identify their chemical composition.

2.3.3. Thermogravimetric analysis

The encapsulation yield of the synthesized PUF-fragrance microcapsules was determined by thermogravimetric analysis (TGA/SDTA 851 Mettler Toledo), comparing microcapsules with different dosage (ml) of fragrances: M30, M45 and M60 (mint fragrance) and C30, C45 and C60 (cuir fragrance). The test was conducted in N_2 atmosphere from room temperature to 800ºC with a heating rate of 10ºC/min. The initial weight is set after establishing an inert atmosphere. Next the desired heating program is started and the specimen weight continuously monitored in the recorder. The ordinate setting can be either weight in milligrams or percentage of the original sample weight. The corresponding 1^{st} derivative of the TGA curve, dTGA, provides the decomposition rate.

2.3.4. Ultraviolet-visible spectroscopy

To contrast the results obtained by thermogravimetric analysis and thereby validate the technique, the yield percentage was also determined by ultraviolet-visible spectroscopy (UV-240 LPC, Shimadzu).

A sample of the resultant slurry is introduced into the centrifuge. Once separated in two phases, an aliquot is extracted and taken to a volume of 50ml with monacol. A homogeneous sample of the solution will be analyzed in the UV-Visible. This methodology was repeated for different dosages of mint fragrance (30, 60 and 90 ml).

3. Results and discussion

3.1. Synthesis of PUF-fragrance microcapsules

Fragrance was encapsulated in PUF through in-situ polymerization. Figure 7 illustrates the process with reactants and products.

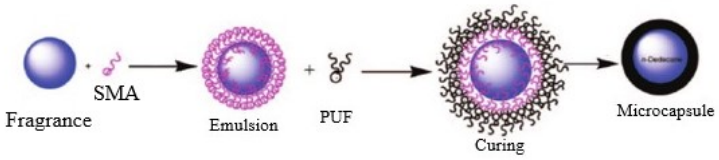

Figure 7. Schematic representation of in-situ polymerization of UF resin for encapsulation of fragrance [33].

With the help of the high-performance dispersing instrument and the EMA aqueous solution as a stabilizer, fragrance could be uniformly suspended in the water phase to form stable oil in water emulsion. Upon heating at 70ºC with pH at 8-9, urea and formaldehyde started to polymerize and, finally, PUF form a solid plastic shell surrounding the fragrance droplets suspended in the aqueous phase.

Fragrance residual and unreacted formaldehyde on the microcapsule surface will cause coalescence between microcapsules, resulting in heavy agglomeration of microcapsules.

To avoid these situations, we used ammonium chloride solution as the final washing solvent to remove the excessive fragrance and unreacted formaldehyde, which turned out to be an efficient method to obtain a loose powder form of microcapsules. The reaction between ammonium chloride and formaldehyde, therfore, allows reduction of unwanted free formaldehyde.

$$4NH_4Cl + 6HCHO \leftrightarrows (CH_2)_6N_4 + 4HCl + 6\ H_2O$$

3.2. Characterization of PUF-fragrance microcapsules

3.2.1. Morphology of synthesized microcapsules

The optical microscope was used to observe the size and morphology of synthesized microcapsules. The diameter of the mint microcapsules was (4.40 ± 3.30) µm (Figure 8) and (3.75 ± 1.75) µm the cuir microcapsules (Figure 9), which is relatively uniform. The surface of the microcapsules is rough and it can be appreciated an important presence of sub-species located in the microcapsule wall according to the SEM image.

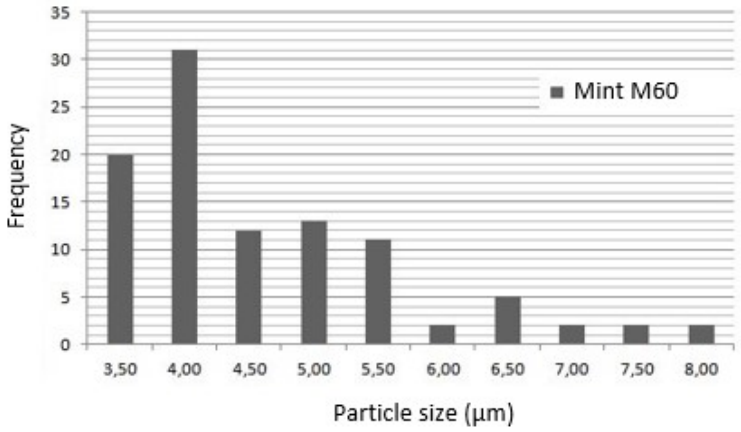

Figure 8. Size distribution of mint microcapsules synthesized.

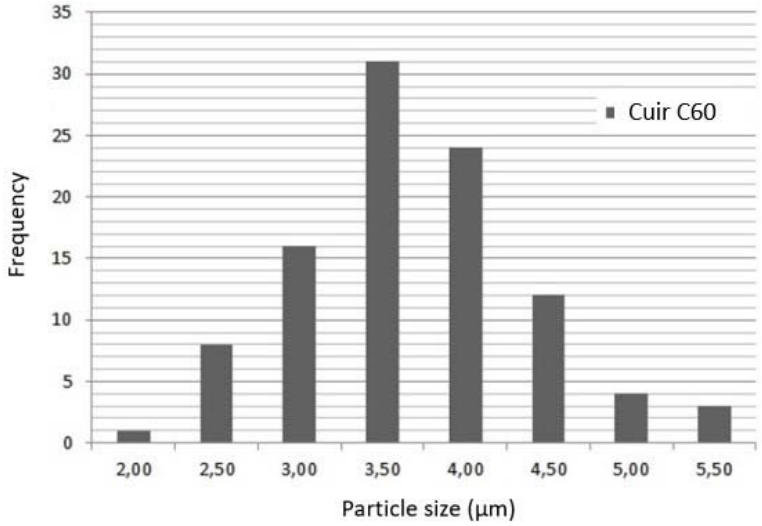

Figure 9. Size distribution of cuir microcapsules synthesized.

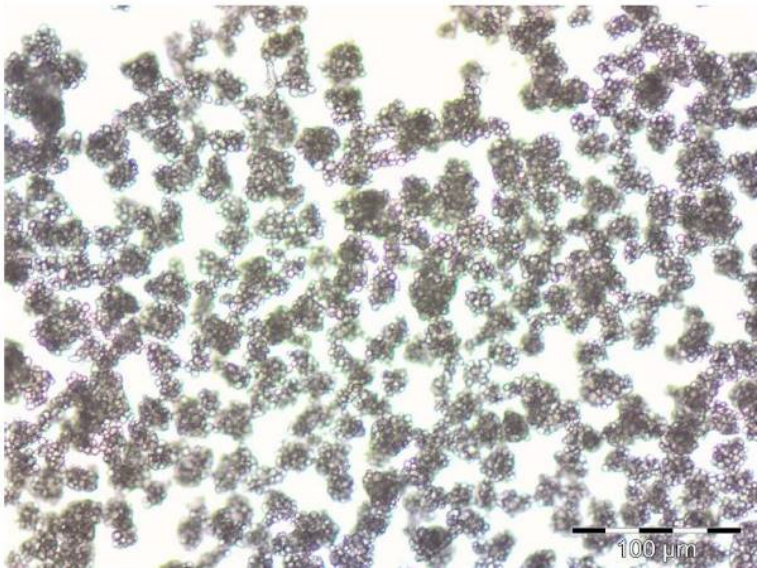

Figure 10. Optical microscope image of mint microcapsules synthesized.

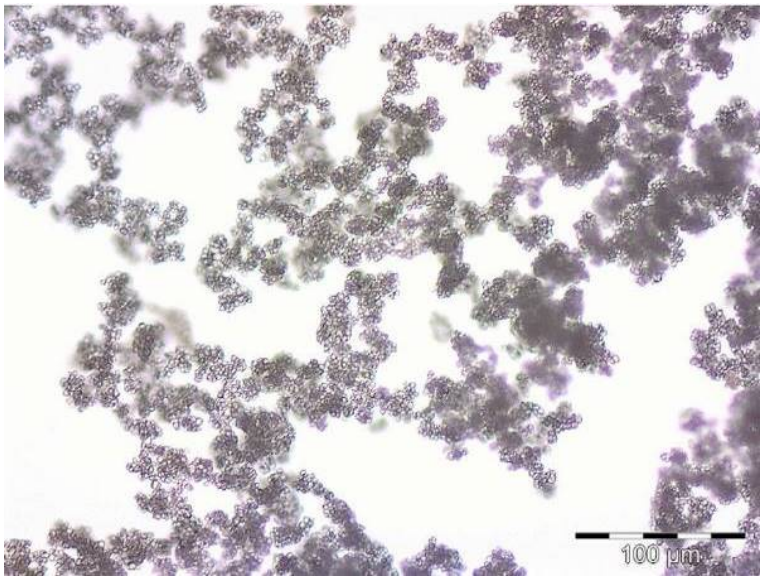

Figure 11. Optical microscope image of cuir microcapsules synthesized.

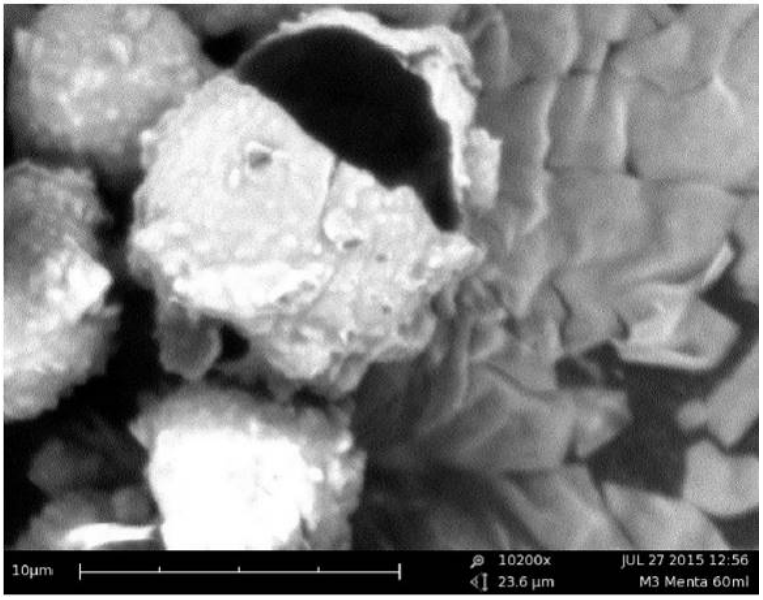

Figure 12. SEM image of mint microcapsules synthesized.

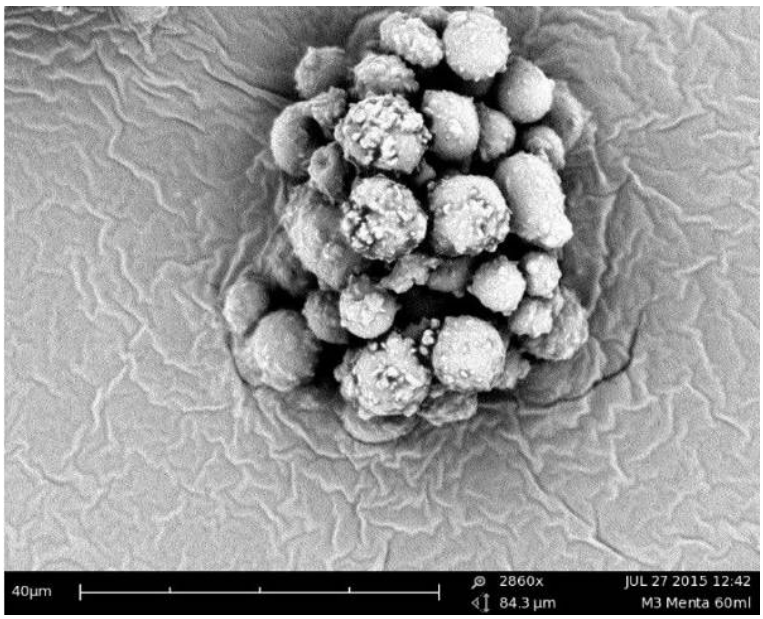

Figure 13. SEM image of mint microcapsules synthesized.

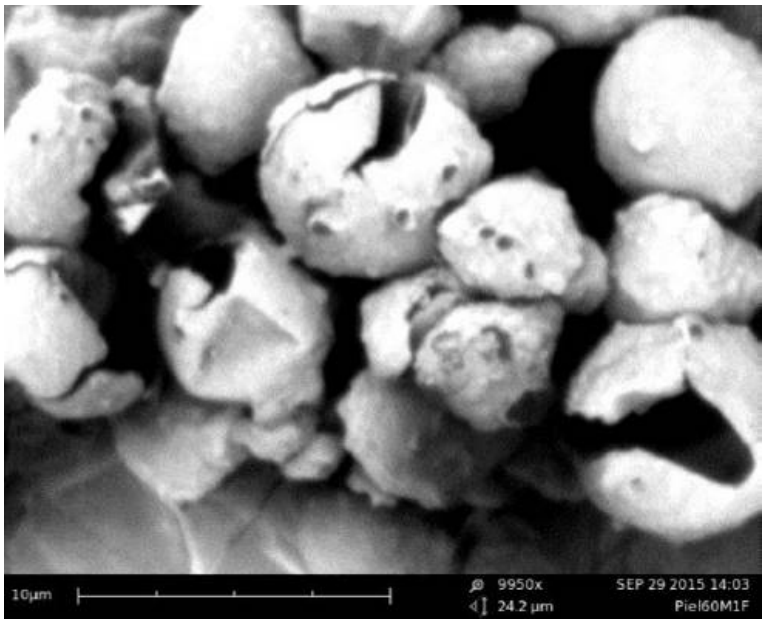

Figure 14. SEM image of cuir microcapsules synthesized.

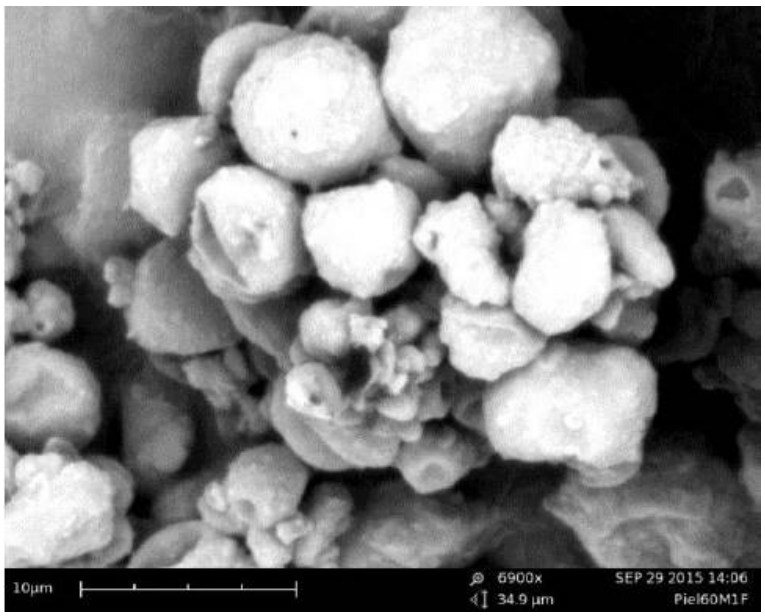

Figure 15. SEM image of cuir microcapsules synthesized.

3.2.2. Fourier transform infrared spectroscopy

In order to prove that the microcapsules were successfully synthesized, we adopted, as example, mint microcapsules FTIR to identify the chemical composition of the synthesized microcapsules. As shown in Figure 16, the FTIR spectra of synthesized microcapsules shows characteristic peak at 3425 cm^{-1}, 2955 cm^{-1} and 1617 cm^{-1} which were assigned to the stretching vibration absorption of secondary N-H, -CH, and C=O respectively [34]. The peak of amide functional group is located at 1670 cm^{-1}. Finally, there are also the characteristic bands of tertiary amines between 1350 and 1200 cm^{-1} [35].

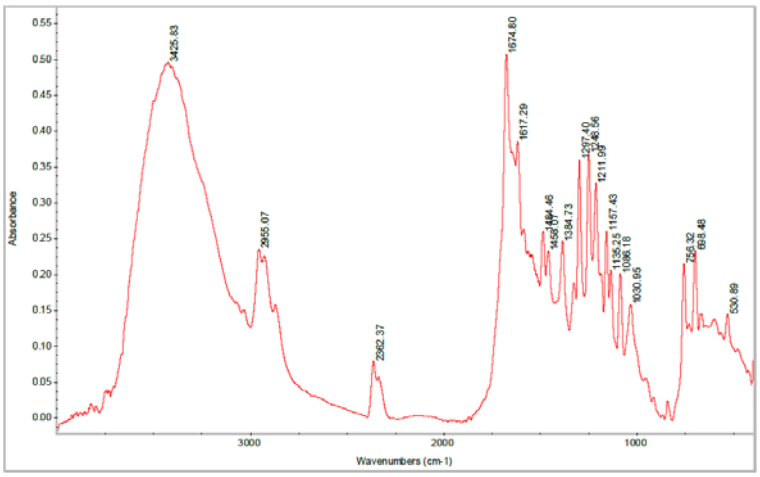

Figure 16. FTIR spectra of M60.

In the FTIR spectra of pure urea (Figure 17), the characteristic peak of the -CH group is

reduced from 0.24 to 0.08 and the characteristic peak of amide is raised from 0.5 to 1.0. Thus, the FTIR result further proved that the mint fragrance was successfully encapsulated in the PUF shell.

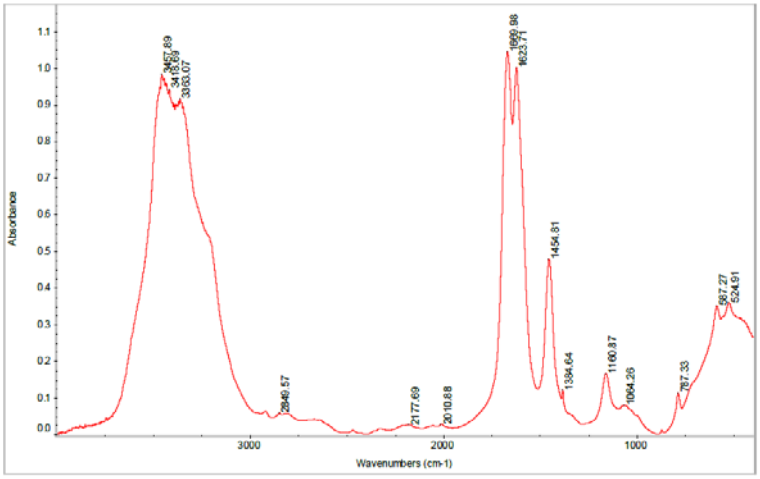

Figure 17. FTIR spectra of pure urea.

3.2.3. Thermogravimetric analysis

Previously, other methods have been used to quantify the capsule core content: soxhlet extraction [36], [37], sonicated-filtration determination [38], drug delivery by ultraviolet–visible (UV–Vis) spectroscopy [39], [40], elemental analysis using a Carbon-Hydrogen-Nitrogen (CHN) analyser [41] or a simple dry residue determination [42]. In this research, to quantify the content of core material in the microcapsules, we adopted thermogravimetric analysis to evaluate the mass percentage of mint/cuir fragrance in the product.

TGA and dTGA curves of the mint/cuir fragrance–PUF microcapsules with different dosage of fragrance were displayed from Figure 19 to Figure 22, where the only variation was in fragrance wt%, keeping all other process parameters constant.

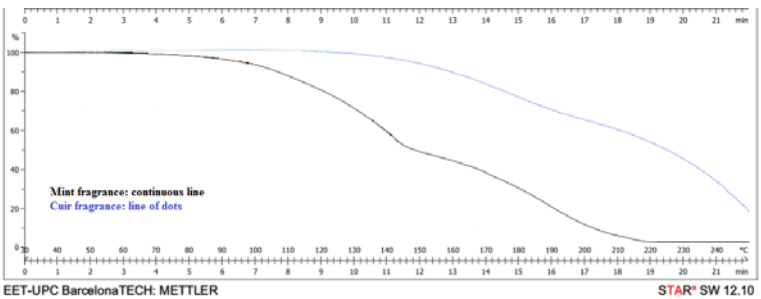

Figure 18. TGA curves for mint and cuir fragrances.

Degradation of mint fragrance starts at about 80ºC and cuir fragrance started to decompose at 130ºC (Figure 18), which shows that these oils have high volatility and requires protection for application on surfaces that aim for high durability.

The TGA and dTGA mint fragrance–PUF microcapsules curves (Figure 19) showed that PUF started to decompose around 198 ºC (T_{onset}) [42], and its weight sharply decreased from 90-82 to 55-41% between 198 and 246 ºC (T_{offset}) with a dTGA minimum at 236ºC (T_{peak}). Within this range, the shell wall degrades and the core material evaporates immediately (take in account that the boiling point of the mint fragance is around 80ºC (Figure 18)).

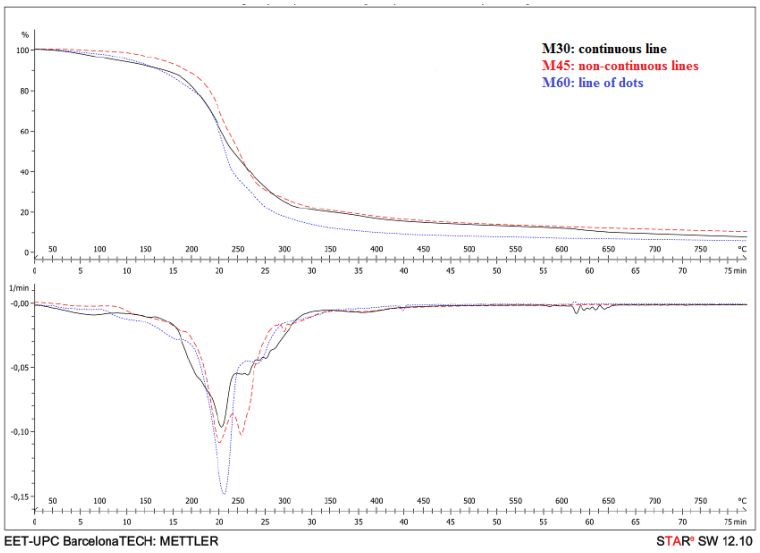

Figure 19. TGA and differential TGA curves for mint fragrances microcapsules.

On the other hand, the TGA and dTGA cuir fragrance–PUF microcapsules curves (Figure 20) show that PUF started to descompose around 177 ºC (T_{onset}), and its weight abruptly decreased from 97-81 to 57-37% between 177 and 252 ºC (T_{offset}) with a dTGA minimum at 236ºC (T_{peak}). As it happened in the case of mint fragrance, within this range, the shell wall degrades and releases the nucleus.

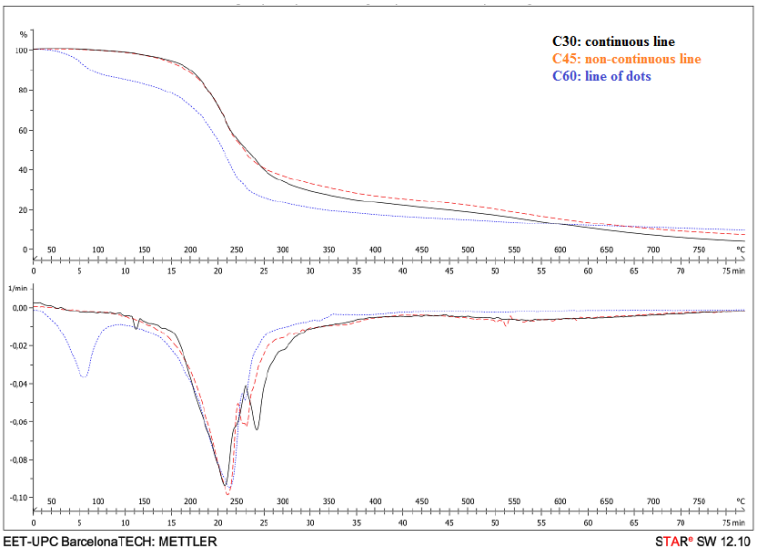

Figure 20. TGA and differential TGA curves for cuir fragrances microcapsules.

It can be observed from Figure 21 that the decomposition rate of the mint fragrances increases in each step as the content of mint fragrance in the system does it too from 0,10 to 0,15 min^{-1}, the same way as the area under the curve increases from 3,58 to 3,98 mg (Table 1). The phenomenon of subspecies formation can also be observed in M30 and M45 batches with the presence of numerous secondary peaks exceeded the 245 ºC.

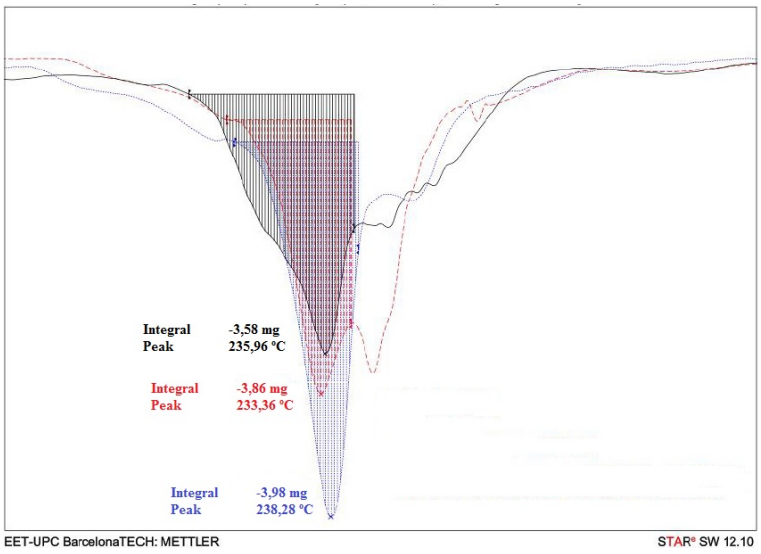

Figure 21. Differential TGA curves for mint fragrances microcapsules. Augmented areas.

Nevertheless, it can be detected from Figure 22 a different behavior for cuir fragrance–PUF microcapsules. In this case, decomposition rate and the area under dTGA curve of different

batches are not in a logical order. This is due to the presence of moisture in the C60 sample (from 38 to 160 ºC), which makes the C60 decomposition rate reaches only 0,097 min^{-1} and the area under the curve 4,07 mg. However, if the area of moisture is taken into account, the resultant area and the decomposition rate would be greater than the C30 and C45 batches (Table 1). In this case, the presence of subspecies can also be clearly observed.

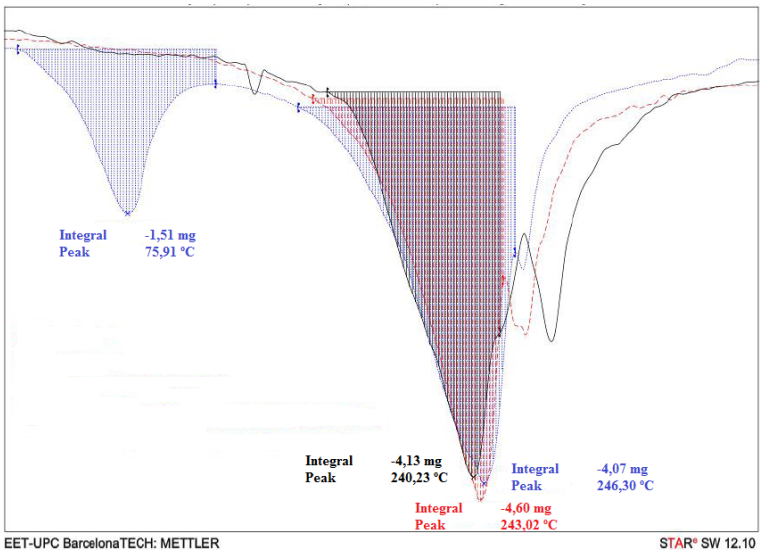

Figure 22. Differential TGA curves for cuir fragrances microcapsules. Augmented areas.

These two cases show that thermogravimetric analysis can be used as a rigorous quantitatively technique to compare the content of core material encapsulated for different batches.

Table 1. Decomposition rate and area under dTGA curves.

Sample	T_{onset} (ºC)	T_{peak} (ºC)	T_{offset} (ºC)	Microcapsules decomposition rate (min^{-1})	Area under dTGA curve (mg)	Process yield (%)
M30	210	236	244	0,100	3,58	30
M45	194	233	244	0,110	3,86	35

M60	190	238	250	0,150	3,98	45
C30	182	240	248	0,094	4,13	40
C45	178	243	251	0,098	4,60	41
C60	**Peak 1** 38	76	124	0,038	1,51	48
	Peak 2 170	246	256	0,092	4,07	

From Table 1, it can be observed in 'area under dTGA curve' column that cuir microcapsules have been able to encapsulate more fragrance than mint microcapsules. As previously mentioned, it can also be seen how, as the fragrance content increases in both cases, so too do decomposition rate and area under the dTGA curve. Therefore, by analysing these two parameters for each batch produced under identical conditions is relatively simple to control the yield percentage of the amount of the fragrance encapsulated, as well as any subspecie formed.

3.2.4. Ultraviolet-visible spectroscopy

The efficiency of encapsulation was obtained indirectly by following the methodology presented in section 2.3.4.

The supernatant of three centrifuged samples of mint fragrance–PUF microcapsules batches were analysed by ultraviolet-visible spectroscopy. The result of the analyses with the three different dosages (30, 60 and 90 ml) must give an account of the mint fragrance that has been encapsulated with respect to the fragrance introduced in the reactor initially.

The results obtained with this method are presented in the following Table 2 along with the results obtained using TGA method.

Table 2. Process yield with TGAmethod and UV-visible method.

Sample	Process yield (%)	
	TGA method	UV-visible method
	Oil encapsulated/weight of filtered and dried microcapsules	Oil encapsulated/oil added to the reactor
M30	30,000	99,722
M45	35,000	99,892
M60	45,000	99,998

It can be observed how the yields are directly proportional to the fragrance added to the reactor (30, 40, 60ml) for both TGA method and UV-visible methods. In this way, the success of the new method is shown with these results.

4. Conclusion

In this study, a series of PUF microcapsules containing mint and cuir fragrance with various mass ratios were successfully synthesized via in-situ polymerization in the oil-in-water emulsion. A set of characterization methods of the synthesized microcapsules was used to confirm their chemical composition and morphology. FTIR spectrum proved that the microcapsules were created. Optical microscope and SEM observations further confirmed the spherical morphology of the microcapsules. The results of the thermogravimetric analysis have successfully showed that they can be used as a quantitatively technique to compare the content of core material encapsulated for different batches. Therefore, this study shows that the more quantity of fragrance is encapsulated, the better quality is the microcapsule morphologically. Finally, there was a clear link between the decomposition rate of the core material, area under dTGA curve and the amount of core material encapsulated. The success of the new TGA method is shown by comparing with yields obtained with UV-visible method.

5. References

[1] A. D. Bangham, R. W. Horne, J. Mol. Biol. 1964, 8, 660.

[2] A. D. Bangham, M. M. Standish, G. Weissman, J. Mol. Biol. 1965, 13, 253.

[3] Martí, M., Rodríguez, R., Carreras, N., Lis, M., Valldeperas, J., Coderch, L. and Parra, J. (2012). Monitoring of the microcapsule/liposome application on textile fabrics. Journal of the Textile Institute, 103(1), pp.19-27.

[4] Martí, M., Barsukov, L., Fonollosa, J., Parra, J., Sukhanov, S., Coderch, L. (2004). Physicochemical Aspects of the Liposome-Wool Interaction in Wool Dyeing. Journal of American Chemical Society, 20, 3068-3073.

[5] H. Surburg, J. Panten, Common Fragrance and Flavor Materials: Preparation, Properties and Uses, 6th ed., Wiley-VCH, Weinheim 2016.

[6] G. Ohloff, W. Pickenhagen, P. Kraft, Scent and Chemistry, Wiley-VCH, Weinheim 2011.

[7] S.-J. Park, R. Arshady, Microspheres, Microcapsules Liposomes 2003, 6, 157.

[8] G. Y. Zhu, Z. B. Xiao, R. J. Zhou, F. P. Yi, Adv. Mater. Res. 2012, 535–537, 440.

[9] R. Ciriminna, M. Pagliaro, Chem. Soc. Rev. 2013, 42, 9243.

[10] D. L. Berthier, N. Paret, A. Trachsel, A. Herrmann, Bioconjugate Chem. 2010, 21, 2000.

[11] H. Morinaga, H. Morikawa, Y. Wang, A. Sudo, T. Endo, Macromolecules 2009, 42, 2229.

[12] D. L. Berthier, I. Schmidt, W. Fieber, C. Schatz, A. Furrer, K. Wong, S. Lecommandoux, Langmuir 2010, 26, 7953.

[13] G. Kreutzer, C. Ternat, T. Q. Nguyen, C. J. G. Plummer, J.-A. E. Månson, V. Castelletto, I. W. Hamley, F. Sun, S. S. Sheiko, A. Herrmann, L. Ouali, H. Sommer, W. Fieber, M. I. Velazco, H.-A. Klok, Macromolecules 2006, 39, 4507.

[14] M. Jacquemond, N. Jeckelmann, L. Ouali, O. P. Haefliger, J. Appl. Polym. Sci. 2009, 114, 3074.

[15] M. A. Teixeira, O. Rodríguez, S. Rodrigues, I. Martins, A. E. Rodrigues, AIChE J. 2012, 58, 1939.

[16] M. Pretzl, M. Neubauer, M. Tekaat, C. Kunert, C. Kuttner, G. Leon, D. Berthier, P. Erni, L. Ouali, A. Fery, ACS Appl. Mater. Interfaces 2012, 4, 2940.

[17] A. V. Sadovoy, M. V. Lomova, M. N. Antipina, N. A. Braun, G. B. Sukhorukov, M. V. Kiryukhin, ACS Appl. Mater. Interfaces 2013, 5, 8948.

[18] N. Paret, A. Trachsel, D. L. Berthier, A. Herrmann, Angew. Chem., Int. Ed. 2015, 54, 2275.

[19] I. Hofmeister, K. Landfester, A. Taden, Macromolecules 2014, 47, 5768.

[20] I. Hofmeister, K. Landfester, A. Taden, Angew. Chem., Int. Ed. 2015, 54, 327.

[21] Panisello, C., Peña, B., Gumí, T. and Garcia-Valls, R. (2012). Polysulfone microcapsules with different wall morphology. Journal of Applied Polymer Science, 129(3), pp.1625-1636.

[22] L. Cahn and H. Schultz, Anal. Chem. 35, 1729 (1963).

[23] R. C. Mackenzie, in I. M. Kolthoff, P. J. Elving, and E. B. Sandell, eds., Treatise on Analytical Chemistry, Vol. 12, Pt. 1, John Wiley & Sons, Inc., New York, 1983, p. 1.

[24] J. O. Hill, For Better Thermal Analysis and Calorimetry, ICTA, 3rd ed., CPC Reprographics, Portsmouth, U.K., 1991.

[25] P. K. Gallagher, Adv. Anal. Geochem. 1, 211 (1993).

[26] Xiao, Z., Zhang, Y., Zhu, G., Niu, Y., Xu, Z., & Zhu, J. (2017). Preparation of micro-encapsulated strawberry fragrance and its application in the aromatic wallpaper. Polish Journal of Chemical Technology, 19(1), 89-94. https://doi.org/10.1515/pjct-2017-0013

[27] Sarkar, S., & Kim, B. (2017). Analysis of graphene-encapsulated polymer microcapsules with superior thermal and storage stability behavior. Polymer Degradation and Stability, 138, 72–81. https://doi.org/10.1016/j.polymdegradstab.2017.02.012

[28] Yu, X., Qi, H., Huang, Z., Zhang, B., & Liu, S. (2017). Preparation and characterization of spherical β-cyclodextrin/urea-formaldehyde microcapsules modified by nano-titanium oxide. RSC Advances, 7(13), 7857–7863. https://doi.org/10.1039/c6ra27895g

[29] Vallejos, S. (2010). Estudio de la reducción de emisión de formaldehído en las resinas de urea formaldehído, 5–7.

[30] Rochmadi (2010). Mechanism of Microencapsulation with Urea-Formaldehyde Polymer. American Journal of Applied Sciences, 7(6), pp.739-745.

[31] Quimica.laguia2000.com (2017). Polimerización – Polímeros de Condensación | La Guía de Química. [Accessed 19 Oct. 2017].

[32] C.J. Fan, X.D. Zhou, Influence of operating conditions on the surfacemorphology of microcapsules prepared by in situ polymerization, ColloidsSurf. A 363 (2010) 49–55.

[33] Zhu, K., Qi, H., Wang, S., Zhou, J., Zhao, Y., Su, J. and Yuan, X. (2012). Preparation and Characterization of Melamine-Formaldehyde Resin Micro- and Nanocapsules Filled withn-Dodecane. Journal of Macromolecular Science, Part B, 51(10), pp.1976-1990.

[34] Qin, R., Xu, G., Guo, L., Jiang, Y. and Ding, R. (2012). Preparation and characterization of a novel poly(urea–formaldehyde) microcapsules with similar

reflectance spectrum to leaves in the UV–Vis–NIR region of 300–2500 nm. Materials Chemistry and Physics, 136(2-3), pp.737-743.

[35] G. Socrates, Infrared and Raman Characteristic Group Frequencies Tables andCharts, third ed., John Wiley & Sons, New York, 2001.

[36] Ting, Z., Min, Z., Xiao-Mei, T., Feng, C. and Jian-Hui, Q. (2009). Optimal preparation and characterization of poly(urea-formaldehyde) microcapsules. Journal of Applied Polymer Science, 115(4), pp.2162-2169.

[37] Thanawala, K., Mutneja, N., Khanna, A. and Raman, R. (2014). Development of Self-Healing Coatings Based on Linseed Oil as Autonomous Repairing Agent for Corrosion Resistance. Materials, 7(11), pp.7324-7338.

[38] Es-haghi, H., Mirabedini, S., Imani, M. and Farnood, R. (2014). Preparation and characterization of pre-silane modified ethyl cellulose-based microcapsules containing linseed oil. Colloids and Surfaces A: Physicochemical and Engineering Aspects, 447, pp.71-80.

[39] Bezerra, F., Carmona, O., Carmona, C., Lis, M. and de Moraes, F. (2016). Controlled release of microencapsulated citronella essential oil on cotton and polyester matrices. Cellulose, 23(2), pp.1459-1470.

[40] Wang, B., Adhikari, B. and Barrow, C. (2014). Optimisation of the microencapsulation of tuna oil in gelatin–sodium hexametaphosphate using complex coacervation. Food Chemistry, 158, pp.358-365.

[41] Brown, E., Kessler, M., Sottos, N. and White, S. (2003). In situ poly(urea-formaldehyde) microencapsulation of dicyclopentadiene. Journal of Microencapsulation, 20(6), pp.719-730.

[42] Shirzad, S., Hassan, M., Aguirre, M., Mohammad, L., Cooper, S. and Negulescu, I. (2017). Microencapsulated Sunflower Oil for Rejuvenation and Healing of Asphalt Mixtures. Journal of Materials in Civil Engineering, 29(9), p.04017147.

[43] de la Paz Miguel, M., Ollier, R., Alvarez, V. and Vallo, C. (2016). Effect of the preparation method on the structure of linseed oil-filled poly(urea-formaldehyde) microcapsules. Progress in Organic Coatings, 97, pp.194-202.